Journal of Nano- and Electronic Physics
Vol. **15** No 4, 04039(5pp) (2023)

Журнал нано- та електронної фізики
Том **15** № 4, 04039(5cc) (2023)

Design and Simulation of a Compact Microstrip Antenna for 5G Applications at the (37 – 40) GHz Band

A.S.A. Gaid*, M.A.M. Ali†

Department of Communication & Computer Engineering, Faculty of Engineering and Information Technology, Taiz University, Taiz, Yemen

(Received 24 April 2023; revised manuscript received 23 August 2023; published online 30 August 2023)

This paper proposes a simple, low-profile rectangular microstrip patch antenna for 5G applications in the 37-40 GHz band. The initial design involved a basic rectangular microstrip patch antenna, which was modified to operate efficiently in the target frequency band. The antenna's performance was improved by adjusting the S_{11} and VSWR through an inset feed to improve the matching between the feeding microstrip line and the radiating element. Further improvements were made by inserting two slits, leading to resonating at 37.9 GHz and 39.68 GHz and expanding the impedance bandwidth. The antenna was designed using a 0.381 mm thick Rogers RT/Duroid-5880 substrate with a dielectric constant of 2.2 and a loss tangent of 0.0009. The final design measured $6.11 \times 6 \times 0.381$ mm^3 and achieved minimum S_{11} values of – 32.14 dB and – 17.8 dB at 37.9 GHz and 39.68 GHz, respectively. The antenna also achieved VSWR values of 1.05 and 1.3 at the resonance frequencies. Moreover, an impedance bandwidth of 3.57 GHz extending from 36.65 GHz to 40.22 GHz was achieved. The proposed antenna achieved a maximum gain of approximately 7.98 dBi over frequencies ranging from 37.8 GHz to 38.6 GHz and a minimum of 6.2 dBi at 40.2 GHz. Additionally, the antenna realized a radiation efficiency above 96 % across the operational band. The antenna design, simulations, and optimizations were performed using HFSS, while CST was used to validate the simulation results. The simulation outcomes from both software simulators indicated a high level of agreement.

Keywords: 37-40 GHz band, Compact antenna, Slits, 5G applications.

DOI: 10.21272/jnep.15(4).04039 PACS number: 84.40.Ba

1. INTRODUCTION

The demand for faster data transfer rates and improved network capacity has resulted in lightning-fast advancements in the world of wireless communications. 5G technology is a prime example of this, offering even higher data transfer rates and lower latencies [1, 2]. However, achieving these high data rates requires a wider frequency spectrum, available only in the millimeter wave (mm-Wave) band, which poses some challenges [3-7]. Despite the challenges, the 37-40 GHz frequency band is emerging as a strong contender for the next generation of mobile networks, thanks to its high bandwidth and potential for high-speed transmission. However, signal attenuation due to path losses and absorption by rain, atmospheric gases, and obstacles remain significant hurdles that must be overcome [8-10]. To achieve optimal performance in 5G systems, advanced techniques such as beamforming and multiple antennas are employed [11-12].

Microstrip patch antennas (MSPAs) are an excellent fit for millimeter waves and building beamforming arrays due to their compact size and low profile [13]. However, they have certain limitations, such as narrow bandwidth and low gain [13, 14]. Fortunately, there are innovative approaches such as modified patch designs, feeding techniques, and the use of slots and slits, applying DGS, partial ground, and metamaterial techniques that can enhance MSPAs' performance in 5G systems. As a result of these advancements, there is a diverse range of antenna designs suitable for portable devices, smartphones, and beamforming arrays for specific frequencies such as 28, 38/39, and 60 GHz [15-21].

For example, [15] presents a dual-band rectangular patch antenna operating at 38 GHz and 60 GHz, fed via a microstrip line on a Rogers RO3003™ substrate. The antenna has a minimum return loss of 42 dB, a 2 GHz impedance bandwidth at 38 GHz, and a peak gain of 6.5 dBi. Its physical dimensions are $15 \times 25 \times 0.25$ mm^3.

The authors of [16] present a circular microstrip patch antenna with an elliptical slot for 5G mobile communication networks at 28/45 GHz. The antenna has a bandwidth of 1.3 GHz and 1 GHz, efficiency of 85.6 % at 28 GHz and 95.3 % at 45 GHz, and achieves return loss of 40 dB and 7.6 dB maximum gain at 28 GHz, and 14 dB return loss and 7.21 dB maximum gain at 45 GHz. The antenna is built on a $6 \times 6 \times 0.578$ mm^3 Rogers RT5880 substrate with a dielectric constant of 2.2 and loss tangent ($\tan\delta$) of 0.0013.

Paper [17] introduces an HP-shaped antenna for the 36.83 GHz to 40 GHz frequency range. The antenna is built on a $23.7 \times 8.8 \times 0.51$ mm^3 Rogers RT5880 substrate and has a return loss of around 33 dB, maximum gain of 6.5 dBi, 3.17 GHz bandwidth, and over 80 % radiation efficiency.

Sehrai D. A. et al [18] proposed a two-pronged fork-shaped antenna, excited by a microstrip feed line, resonating at 38.5 GHz. The antenna is built on a 10×6 mm^2 Rogers RT5880 substrate with a relative permittivity of 2.2, 0.254 mm thickness, and 0.0009 loss tangent. It has

* quddoos.gaid@taiz.edu.ye
† muhamd.abd.mosud@gmail.com

a return loss of about 30 dB, 7.6 dBi gain, and less than 2 GHz of impedance bandwidth.

In contrast, the researchers in [19] developed a fork-shaped antenna with a quarter-wave transformer feed line to excite the U-shaped arm, resonating at 37 GHz. The antenna is built on a 10 x 6 mm² Rogers RT5880 substrate with a relative permittivity of 2.2, 0.254 mm thickness, and 0.0009 loss tangent. It has a return loss of about 20 dB, 6.84 dBi gain, and approximately 1 GHz of impedance bandwidth.

The discussion above reveals that some proposed antenna designs suffer from low gain, narrow bandwidth, large dimensions, or a combination of these factors. On the other hand, some high-gain and/or wide bandwidth designs are too bulky for integration into smartphones or beamforming antenna arrays. This study aims to overcome these limitations by developing a compact, high-gain antenna with sufficient impedance bandwidth to cover the 37 GHz to 40 GHz range. The antenna is designed, simulated, and optimized using HFSS, and the simulation results are verified using CST. The rest of the paper is organized as follows: Section 2 describes the proposed antenna design, Section 3 presents the simulation results, and Section 4 summarizes the conclusions and outlines future directions.

2. THE ANTENNA DEVELOPMENT

The proposed antenna element geometry for use in smartphones, MIMO arrays, or beamforming arrays is depicted in Fig. 1. The radiating element, made of a 0.035 thick copper, is supported by a Rogers RT-5880 substrate with dimensions of 6.11 × 6 × 0.381 mm³. To ensure good performance, a finite ground plane of similar size to the substrate is used to minimize the antenna-radiated wave flow in the backward direction. The dimensions of the optimized antenna element are detailed in Table 1.

The radiating patch antenna is a modified version of the regular rectangular microstrip patch antenna, which has been enhanced by introducing an inset feed to match the microstrip feed line and the radiating patch.

The design process involved four steps to achieve a resonant frequency in the 37-40 GHz mm-wave 5G band. In Fig. 2, the design steps were evaluated, and in Fig. 3, the reflection coefficients were compared. In the first step, using a plain rectangular shape antenna did not cause resonance at the desired frequency and did not yield any bandwidth. In the second step, the match between the microstrip feed line and the radiating patch was improved by implementing the inset feed technique. Fig. 3 clearly shows that the S_{11} performance was significantly enhanced. The resonance occurred at approximately 37.7 GHz with a return loss value of 26.5 dB and an achievable bandwidth of about 2.6 GHz (36.4-39 GHz). In the third step, however, a long slit was inserted into the right side of the radiating element along its length, as shown in Fig. 2.

Unfortunately, the S_{11} performance deteriorated after inserting this long slit. In step 4, another longitudinal slit was added to the left side of the radiating element. This slit separated the left part in a way that the radiating patch became two separate radiating elements, one fed directly through a microstrip feed line and another fed indirectly through electromagnetic induction.

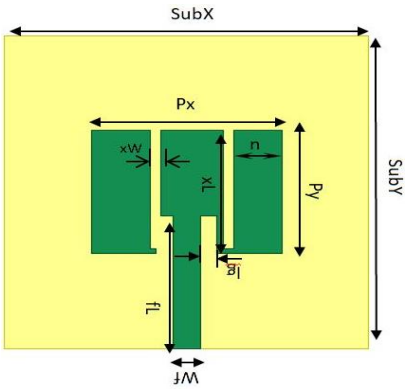

Fig. 1 – Geometry of the proposed antenna

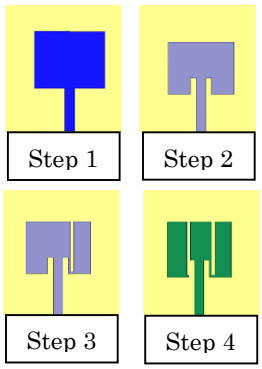

Fig. 2 – The proposed antenna development steps

Fig. 3 depicts the S_{11} performance for the four steps, in which the return loss is notably improved, and the impedance bandwidth is widened to cover the targeted band. The impedance bandwidth now covers the range from 36.65 GHz to 40.22 GHz, and return loss values are quite good, with less than 32 dB achieved at 37.9 GHz and about 17.6 dB at 39.68 GHz.

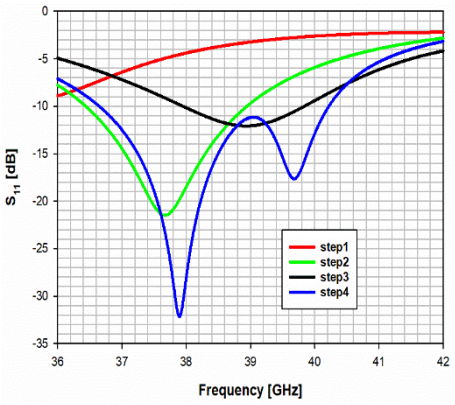

Fig. 3 – S_{11} for the antenna at different design steps (HFSS)

Table 1 – Dimensions of the optimized design

Parameter	Value (mm)	Parameter	Value (mm)
SubY	6.11	**SubX**	6
Py	2.41	**Px**	3.142
Wf	0.45	**fL**	2.583
lg	0.28	**n**	0.78
xL	2.4	**xW**	0.18

3. SIMULATION RESULTS AND DISCUSSION

This section involves the evaluation of the optimized design's performance, including an examination of various aspects such as the antenna's reflection coefficient, 2D radiation characteristics, voltage standing wave ratio (VSWR), surface current distribution, antenna gain, and radiation efficiency. To conduct this assessment, two well-known electromagnetic simulators, HFSS and CST, are utilized. The HFSS simulator is employed for the design and simulation process, and subsequently, the proposed antenna is simulated again using the CST simulator. Comparing the results obtained from both simulators helps to validate the accuracy of the HFSS simulation results, as manufacturing and measurement capabilities are not currently available in our country.

3.1 The Reflection Coefficient

Fig. 4 shows that the simulated results obtained from HFSS and CST are in acceptable agreement, with a small deviation in the resonance frequencies. The red line in the plot represents the S_{11} performance from the HFSS software, indicating that the impedance bandwidth achieved ranges from 36.65 GHz to 40.22 GHz, with a minimum return loss value of less than 32.14 dB at 37.9 GHz and near 17.8 dB at 39.68 GHz. Conversely, the black line represents the S_{11} performance obtained from the CST software, with the – 10 dB realized impedance bandwidth extending from approximately 36.2 GHz to 39.7 GHz, and return loss values of 24 dB at 37.3 GHz and about 19.5 dB at 39.1 GHz. Despite a slight deviation, the two curves are quite similar.

3.2 The VSWR

Fig. 5 displays the VSWR performance of the proposed antenna as predicted by HFSS and CST software packages. The HFSS-generated VSWR curve shows values of 1.05 and 1.3 at frequencies of 37.9 GHz and 39.68 GHz, respectively (shown by the red curve). Furthermore, the black curve obtained from the CST software indicates VSWR values of approximately 1.14 and 1.24 at frequencies of 37.26 GHz and 39.11 GHz, respectively. The two curves demonstrate good similarity, indicating agreement between the results obtained from the two software packages. The impedance bandwidth obtained for VSWR ≤ 2 is shown to cover the frequency band from 36.65 GHz to 40.22 GHz (as indicated by the red line curve) while covering the range extending from 36.18 GHz to 39.68 GHz as predicted by CST (see the black curve). This agreement between the bandwidths obtained from the S_{11} curves and VSWR curves highlights the consistency of the simulation results.

3.3 Radiation Characteristics

The gain of an antenna is a crucial performance factor that reflects its radiation efficiency and directivity. Fig. 6 (a, b) presents the 2D radiation patterns at 38 GHz for phi = 0° and phi = 90° and exhibits good consistency between the simulated patterns obtained from both simulators. The maximum gain value as predicted by HFSS is 7.98 dBi, while that predicted by CST is 7.53 dBi. As shown in Fig. 6, the radiation patterns obtained from the two simulators are in good agreement.

Fig. 7 depicts the proposed antenna's gain and radiation efficiency as a function of operating frequencies. Both graphs were generated using HFSS and show that the antenna achieves a maximum gain of 7.98 dBi over frequencies ranging from 37.8 GHz to 38.6 GHz. At 40.2 GHz, the gain reduces to a minimum of 6.2 dBi. Furthermore, according to the HFSS simulation, the antenna has a minimum radiation efficiency of 96 %. However, the CST software predicts a minimum radiation efficiency of approximately 82 %. The 2D and 3D radiation patterns obtained from the two simulators demonstrate good agreement.

3.4 Surface Current Distribution

Surface current distribution is a critical parameter that plays a significant role in determining an antenna's radiation pattern and efficiency, as it represents the varying flow of electric current on the antenna's surface. Fig. 8 shows that the surface current density is primarily concentrated on the feed line, especially the part in the inset feed. Additionally, the current density is focused on the left and bottom edges around the inset of the central part of the patch that is connected with the feed line, and the right edge of the separate part of the antenna. In these regions, the current density ranges from approximately 140 A/m to 150 A/m. In contrast, the current density in the middle of the central part, the rest of the feed line, and the inner right and left edges of the separated part of the patch ranges from approximately 54 A/m to 97 A/m. This current distribution was observed at 38 GHz.

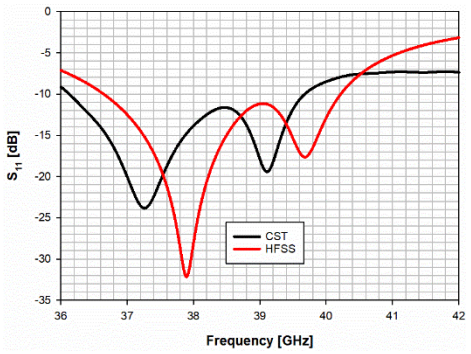

Fig. 4 – The return loss performance of the proposed design using HFSS and CST

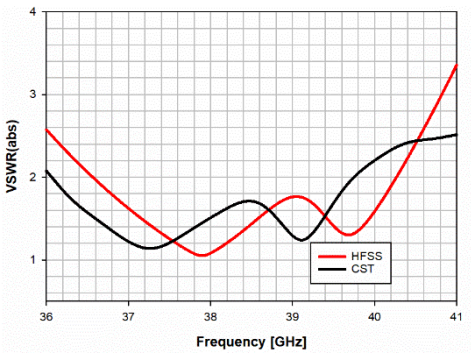

Fig. 5 – The VSWR performance of the proposed design using HFSS and CST

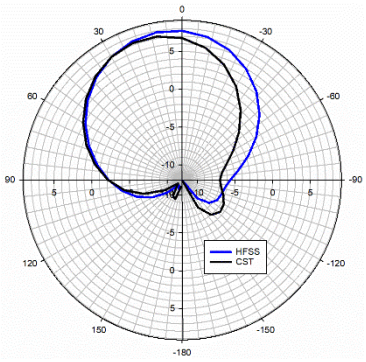

a

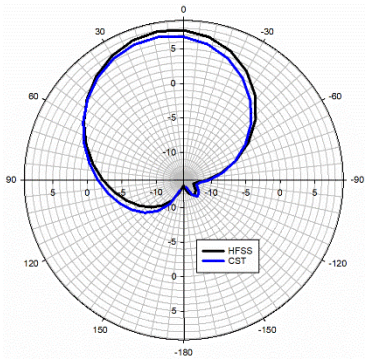

b

Fig. 6 – The 2D radiation patterns of the proposed design at 38 GHz using HFSS and CST: phi = 0° (a) and phi = 90° (b)

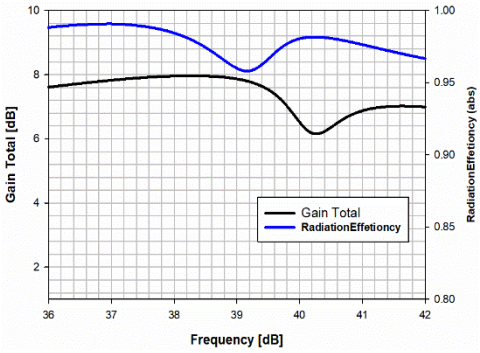

Fig. 7 – The antenna gain and radiation efficiency vs operating frequencies (HFSS)

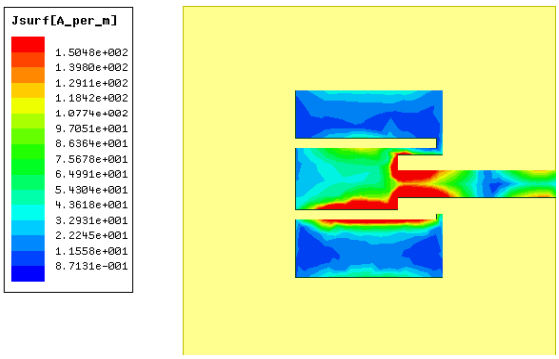

Fig. 8 – The surface current distribution at 38 GHz (HFSS)

3.5 Summary of the Simulation Outcomes

Table 2 provides a summary of the simulation outcomes obtained from both HFSS and CST software. The results obtained from both simulators exhibit a high degree of similarity, indicating a high level of accuracy in the design and optimization of the antenna.

Table 2 – Summary of the simulation outcomes obtained from both simulators

S/W	HFSS		CST	
f_r (GHz)	37.9	39.68	37.26	39.11
S_{11} (dB)	32.14	17.6	23.9	19.40
VSWR	1.05	1.30	1.14	1.24
Gain (dBi)	7.98	7.25	7.24	7.42
Dir. (dB)	8.05	7.45	7.91	8.25
Rad. Eff. (%)	99	96	85	82
BW (GHz)	36.65-40.22		36.18-39.68	

3.6 Comparison with Some Published Works

Table 3 offers a thorough comparison of the proposed antenna in this paper with several recent publications, considering various performance metrics such as antenna size, S_{11}, impedance bandwidth, gain, and radiation efficiency. The comparison reveals that the proposed antenna surpasses all antennas presented in references [15] and [17-19] in terms of antenna size, impedance bandwidth, and gain. Additionally, the proposed design achieves smaller better S_{11} values when compared to the antennas presented in [18] and [19]. The proposed design strikes a balance between bandwidth, gain, and size, making it a superior choice compared to the other designs evaluated in the comparison.

Table 3 – Comparison of the proposed antenna with some other published works

Ref.	**[15]**	**[17]**	**[18]**	**[19]**	**This Work**
Ant. Size mm^3	15 × 25 × 0.25	23.7 × 8.8 × 0.51	10 × 6 × 0.254	10 × 6 × 0.254	6.11 × 6 × 0.381
Sub. Mat.	Rogers RO3003™	Rogers RT5880	Rogers RT5880	Rogers RT5880	Rogers RT5880
Freq GHz	38, 60	38.5	38.5	37	37.9, 39.68
S_{11} dB	42 (@ 38)	– 33	– 30	– 20	– 32.14 – 17.6
Gain dBi	6.5	6.5	7.6	6.84	7.98
BW GHz	2	3.17	≤ 2	≈1	3.57
Rad. Eff. %	89.57	80	N/A	N/A	≥ 82

4. CONCLUSION

This paper introduced a simple and compact rectangular microstrip patch antenna with two longitudinal slits, aiming at 5G applications in the 37-40 GHz frequency range. The proposed design achieves improved performance by adjusting the S_{11} and VSWR through an inset feed and inserting two slits, resulting in a minimum S_{11} of – 32.14 dB and – 17.8 dB at 37.9 GHz and

39.68 GHz, VSWR values of 1.05 and 1.30 at the resonance frequencies, and impedance bandwidth of 3.57 GHz extending from 36.65 GHz to 40.22 GHz. The antenna design, simulations, and optimizations were performed using HFSS; with the simulation results validated using CST. The outcomes obtained from both simulators showed a good level of agreement, indicating the accuracy and effectiveness of the proposed antenna design. The proposed design is compact and suitable for integration into smartphones and handheld devices, as well as MIMO antennas and beamforming antenna arrays in the aforementioned frequency range. Future work will involve the fabrication of the antenna and validation of the design through real measurements.

REFERENCES

1. R.N. Mitra, D.P. Agrawal, *ICT Express* **1** No 3, 132 (2015).
2. P. Pirinen, *1st International Conference on 5G for Ubiquitous Connectivity (5GU)*, art. No 258061, 17 (Akaslompolo: IEEE: 2014).
3. A.N. Uwaechia, N.M. Mahyuddin, *IEEE Access* **8**, 62367 (2020).
4. L. Wei, R.Q. Hu, Y. Qian, G. Wu, *IEEE Wireless Commun.* **21** No 6, 136 (2014).
5. Y. Niu, Y. Li, D. Jin, L. Su, A.V. Vasilakos, *Wireless Netw.* **21**, 2657 (2015).
6. W. Hong, Z. H. Jiang, C. Yu, D. Hou, H. Wang, C. Guo, Y. Hu, L. Kuai, Y. Yu, Z. Jiang, Z. Chen, J. Chen, Z. Yu, J. Zhai, N. Zhang, L. Tian, F. Wu, G. Yang, Z. Hao, J.Y. Zhou, *IEEE J. Microwave.* **1** No 1, 101 (2021).
7. T.S. Rappaport, S. Sun, R. Mayzus, H. Zhao, Y. Azar, K. Wang, G.N. Wong, J.K. Schulz, M. Samimi, F. Gutierrez, *IEEE Access* **1**, 335 (2013).
8. D. Pimienta-del-Valle, L. Mendo, J. M. Riera, P. Garcia-del-Pino, *Electronics* **9** No 11, 1867 (2020).
9. H. Wang, P. Zhang, J. Li, X. You, *China Commun.* **16** No 5, 1 (2019).
10. D. Pimienta-del-Valle, S. Hernández-Sáenz, P. Sáiz-Coronado, L. Mendo, P. Garcia-del-Pino, J. M. Riera, *13th European Conference on Antennas and Propagation (EuCAP)*, art. No. 18759904, 1 (Krakow: IEEE: 2019).
11. J. Zhang, X. Yu, K.B. Letaief, *IEEE Open J. Commun. Soc.* **1**, 77 (2019).
12. F.W. Vook, A. Ghosh, T.A. Thomas, *IEEE MTT-S International Microwave Symposium (IMS2014)*, art. No 6848613, 1 (Tampa: IEEE: 2014).
13. A.S.A. Gaid, M.H.M. Qasem, A.A. Sallam, E.Q.M. Shayea, *Innovative Systems for Intelligent Health Informatics: Data Science, Health Informatics, Intelligent Systems, Smart Computing*, 717 (Cham: Springer International Publishing: 2021).
14. A.S.A. Gaid, M.A.S.A. Ali, M.A. Mohammed, A.A.A. Saeed, O.Y.A. Saeed, A.A. Sallam, B. Hawash, *International Conference of Technology, Science and Administration (ICTSA)*, art. No 9406532, 1(Taiz: IEEE: 2021).
15. M.H. Sharaf, A.I. Zaki, R.K. Hamad, M.M.M. Omar, *Sensors* **20** No 9, 2541 (2020).
16. M.I. Khattak, A. Sohail, U. Khan, Z. Barki, G. Witjaksono, *Prog. Electromag. Res. C* **89**, 133 (2019).
17. D.A. Sehrai, M. Asif, N. Shoaib, M. Ibrar, S. Jan, M. Alibakhshikenari, A. Lalbakhsh, E. Limiti, *Electronics* **10** No 11, 1300 (2021).
18. D.A. Sehrai, J. Khan, M. Abdullah, M. Asif, M. Alibakhshikenari, B. Virdee, W.A. Shah, S. Khan, M. Ibrar, S. Jan, A. Ullah, F. Falcone, *Sci. Rep.* **13** No 1, 4907 (2023).
19. J. Khan, S. Ullah, U. Ali, F. A. Tahir, I. Peter, L. Matekovits, *Sensors* **22** No 7, 2768 (2022).
20. A.S.A. Gaid, S.M.E. Saleh, A.H.M. Qahtan, S.G.A. Aqlan, B.A.E. Yousef, A.A.A. Saeed, *International Conference of Technology, Science and Administration (ICTSA)*, art. No 9406546, 1 (Taiz: IEEE: 2021).
21. A.M.H. Aoun, A.A.A. Saeed, A.S.A. Gaid, O.Y.A. Saeed, M.N.G. Mohammed, B. Hawash, *International Conference of Technology, Science and Administration (ICTSA)*, art. No 9406550, 1 (Taiz: IEEE: 2021).

Проектування та моделювання компактної мікросмужкової антени для застосунків 5G у діапазоні (37–40) ГГц

A.S.A. Gaid, M.A.M. Ali

Department of Communication & Computer Engineering, Faculty of Engineering and Information Technology, Taiz University, Taiz, Yemen

У цій роботі описано просту, низькопрофільну прямокутну мікросмужкову антену для додатків 5G у діапазоні 37-40 ГГц. Початкова конструкція передбачала базову прямокутну мікросмужкову антену, яка була модифікована для ефективної роботи в цільовому діапазоні частот. Ефективність антени була покращена завдяки регулюванню S11 і VSWR за допомогою вставного каналу для покращення узгодження між живильною мікросмужковою лінією та випромінюючим елементом. Подальші вдосконалення були зроблені шляхом вставки двох щілин, що призвело до резонування на 37,9 ГГц і 39,68 ГГц і розширення смуги пропускання імпедансу. Антена була розроблена з використанням підкладки Rogers RT/Duroid-5880 товщиною 0,381 мм з діелектричною проникністю 2,2 і тангенсом втрат 0,0009. Остаточна конструкція виміряла 6,11 × 6 × 0,381 мм^3 і досягла мінімальних значень S11 – 32,14 дБ і – 17,8 дБ на 37,9 ГГц і 39,68 ГГц відповідно. Антена також досягла значень КСВ 1,05 і 1,3 на резонансних частотах. Крім того, була досягнута смуга пропускання імпедансу 3,57 ГГц, що розширюється від 36,65 ГГц до 40,22 ГГц. Запропонована антена досягла максимального посилення приблизно 7,98 дБі на частотах від 37,8 ГГц до 38,6 ГГц і мінімального 6,2 дБі на 40,2 ГГц. Крім того, антена реалізувала ефективність випромінювання понад 96 % у робочому діапазоні. Конструкція антени, моделювання та оптимізація були виконані з використанням HFSS, тоді як CST використовувався для перевірки результатів моделювання. Результати моделювання з обох програмних симуляторів показали високий рівень узгодженості.

Ключові слова: Діапазон 37-40 ГГц, Компактна антена, Щілини, Застосунки для 5G.